Hindawi
Advances in Physical Chemistry
Volume 2017, Article ID 6358601, 5 pages
https://doi.org/10.1155/2017/6358601

Research Article

Methylene Blue Photocatalytic Degradation under Visible Irradiation on In_2S_3 Synthesized by Chemical Bath Deposition

William Vallejo, Carlos Díaz-Uribe, and Kathy Rios

Grupo de Fotoquímica y Fotobiología, Universidad del Atlántico, Km 7 Antigua Vía Puerto Colombia, Barranquilla, Colombia

Correspondence should be addressed to William Vallejo; williamvallejo@mail.uniatlantico.edu.co

Received 2 December 2016; Revised 16 February 2017; Accepted 28 February 2017; Published 16 April 2017

Academic Editor: Leonardo Palmisano

In this work, we synthesized In_2S_3 powder through chemical bath deposition method (CBD) in acid medium; we used thioacetamide as sulphide source and $InCl_3$ as indium ion source. X-ray diffraction, diffuse reflection, and Raman spectroscopy measurements were used for In_2S_3 powder physicochemical characterization. Optical analysis indicated that In_2S_3 was active in the visible region of electromagnetic spectrum; it had a band gap of 2.47 eV; the diffraction patterns and Raman spectroscopy suggested that powder had polycrystalline structure. Furthermore, we also studied the adsorption process of methylene blue (MB) on In_2S_3 powder; adsorption studies indicated that the Langmuir model describes experimental data. Finally, photocatalytic degradation of MB was studied under visible irradiation in aqueous solution; besides, pseudo-first-order model was used to obtain kinetic information about photocatalytic degradation; results indicated that the powder catalyst reduces 26% concentration of MB under visible irradiation.

1. Introduction

Nowadays, a subject of great research worldwide is associated with study of different ways to degrade pollutants (e.g., biological and chemical) present into water sources, because they have a negative impact on both quality ground (internal) and surface level of water reserves last reports indicate that more than 2 million tons of pollutants are generated daily in the planet; furthermore, about 1800 millions of people around the world are supplied by a source of water contaminated by biological or chemical pollutant [1]. This is a serious environmental problem and currently is part of an objective study of different research institutes and government agencies. The World Health Organization (WHO) launched an international plan to evaluate water treatment technologies to establish work policy and to analyze new WHO criteria [2, 3].

Conventional water decontamination processes contain (a) the possible self-purification (waterfalls and streams high speed), (b) desorption air, (c) ozone, (d) hydrogen peroxide, (e) potassium permanganate solutions (chemical oxidation), and (f) aerobiological methods; some of these processes achieve the mineralization of species [4, 5]. Precipitation of heavy metal ions is often performed by the addition of coagulants and flocculants; besides, activated carbon and other adsorbents can be used [6–8]. However, these conventional methods do not degrade common recalcitrant organic pollutants in water, such as dyes, antibiotics, and pesticides. Effective removal from aquatic environments is necessary for water purification and conservation and maintaining human and ecological health [9]. Heterogeneous photocatalysis (HP) is an option to degrade different recalcitrant pollutants, because HP is not a selective process; this methodology could act on almost any contaminant under suitable conditions [10]. Conventionally, photocatalyst most studied in this field is titanium dioxide (TiO_2); however despite all the characteristics, TiO_2 has three main drawbacks: (a) fast recombination rate of photogenerated electron-hole pair, (b) low quantum yield in the photocatalytic reactions in aqueous solutions, and (c) high band gap value (3.2 eV, photocatalytic active only under UV-irradiation) [11]. Today, it is common to modify both bulk and surface properties of TiO_2 to solve these problems; some options involve the following: (a) noble metal loading is used to reduce recombination rate of electron-hole pair; (b) both ion implantation and nonmetal doping are applied to reduce band gap of the TiO_2; and (c) sensitization occurs by absorption of natural and/or synthetic organic dyes.

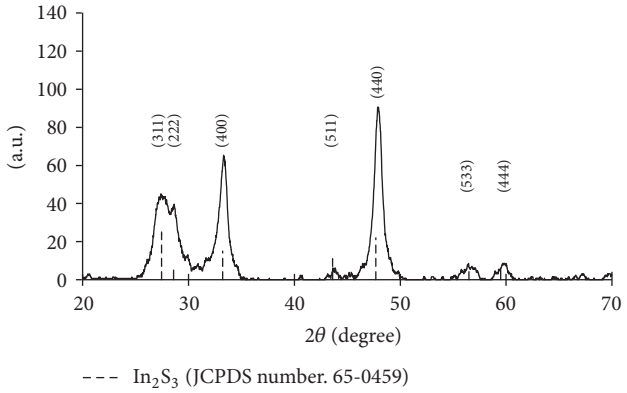

FIGURE 1: XRD pattern of In_2S_3 powder synthesized by CBD process.

These methodologies improve photoactivity of TiO_2 at visible region of electromagnetic spectrum [12]. Another alternative includes change of TiO_2 for other semiconductor having lower band gap value and potential photocatalytic activity; In_2S_3 is considered a promising material due to its chemical stability and its activity in visible range of the electromagnetic spectrum; it has three different crystalline structures and it has potential photocatalytic activity [13–15]. It has been reported that this compound exhibits photocatalytic activity in the degradation of aqueous formic acid and methyl orange under visible light irradiation [16, 17].

The aim of this study is to evaluate the photocatalytic activity of In_2S_3 synthesized by CBD in the degradation of methylene blue as a potential alternative in photocatalysis.

2. Experimental

2.1. Compound Synthesis. Powder of In_2S_3 was synthesized by CBD process from solution containing thioacetamide (Scharlau) (TA: 0.350 M) and indium chloride ($InCl_3$: 0.020 M) as sources of S^{2-} and In^{3+}, respectively; acetic acid (Es-Science) (HA) and sodium citrate (Riedel-de Haën) (Cit: 0.035 M) were used as complexing agents of In^{3+}. The entire reaction can be written as follows:

$$\left[\mathrm{In\,(Ac)}_{4-x}\,\mathrm{HCit}_x\right]_{(ac)} + \mathrm{CH_3SCNH_{2(ac)}} + \mathrm{H_3O^+}_{(ac)} \longrightarrow \mathrm{In_2S_{3(s)}} + x\mathrm{HCit_{(ac)}} + (4-x)\,\mathrm{HAc_{(ac)}} \quad (1)$$

$$+ \mathrm{NCNH_{2(ac)}} + \mathrm{H_2O} \quad (2)$$

All reagents were mixed in pH at 2.5 and temperature at 70°C; after that substrate (soda lime glass) was immersed into reaction reactor and time reaction begins. After reaction finished, solution of reaction was filtered for using filter paper; powder-In_2S_3 was cleaned with bidistilled water; after that, compound was dried on a hot plate at 40°C by 1 hour. After this process we obtained dry powder-In_2S_3.

2.2. Compound Characterization. The optical properties of compound were studied through diffuse reflectance measurements; study was carried out in a Lambda 4 Perkin Elmer spectrophotometer equipped with an integrating sphere. Kubelka-Munk model and analysis based on differential reflection spectra were used to determine independently the energies of the fundamental optical transitions. X-ray diffraction patterns of the samples were recorded in Shimadzu 6000 diffractometer with a source of Cu-K_α radiation (λ = 0.15418 nm) in a range diffraction angle 2θ between 20° and 80°. The Raman spectra were measured in a backscattering configuration at room temperature; the excitation radiation wavelength was 780 nm; the Raman peak analysis is based on Lorentzian-fitting performed in the range of 100–500 cm^{-1}.

2.3. Adsorption Study. All reagents used in this work were of analytical grade. The MB was supplied by Sigma-Aldrich CAS Number 7220-79-3. We provided 4 different concentrations' MB on 0.025 g of In_2S_3. Powder was immersed in each solution and system was magnetically stirred in the dark until reaching the equilibrium of dye adsorption–desorption on In_2S_3 surface; the concentration of MB dye was determined by spectrophotometry (HR2000CG UV-NIR ocean optics) at λ = 665 nm. Content dye of the each solution was determined each five (5) minutes by spectrophotometry; prior to the concentration measurement, samples were filtered through 0.45 mm membrane; all adsorption processes were carried out at 298 K.

2.4. Photocatalytic Activity. In photocatalytic process we used a batch photoreactor under visible irradiation 100 W OSRAM halogen immersion lamp. 0.025 g of In_2S_3 was immersed in the reactor with solution MB (10 ppm); during the photodegradation process, air was injected to reactor; the illumination time was beginning after 60 minutes of dark stirring to reach adsorption equilibrium; finally, the concentration of dye was determined by spectrophotometry at λ = 665 nm.

3. Results and Discussions

3.1. Structural Study. Hydrodynamic synthesis conditions in CBD process (e.g., pH, ion concentration, and temperature) determine both the phase and preferential growth planes of crystalline structure of solid deposited [18]. Figure 1 shows XRD diffraction pattern of powder synthesized by CBD process; preferential growth planes are shown inside figure. XRD pattern shows powder is polycrystalline; besides, main reflections can be assigned to cubic structure of In_2S_3 (JCPDS number 65-0459); it has 4 the preferential growth planes (311), (222), (400), and (440); this result is according to others reposts; this crystalline phase has reported photocatalytic activity for water splitting under visible radiation [19].

3.2. Optical Study. The optical properties of catalyst were determined from diffuse reflectance measurements in the range of 400–900 nm. UV-Vis diffuse reflectance spectra were analyzed with Kubelka-Munk remission function, given by the equation below [20]:

$$F(R_\alpha) = \frac{(1-R_\alpha)^2}{2R_\alpha}, \quad (2)$$

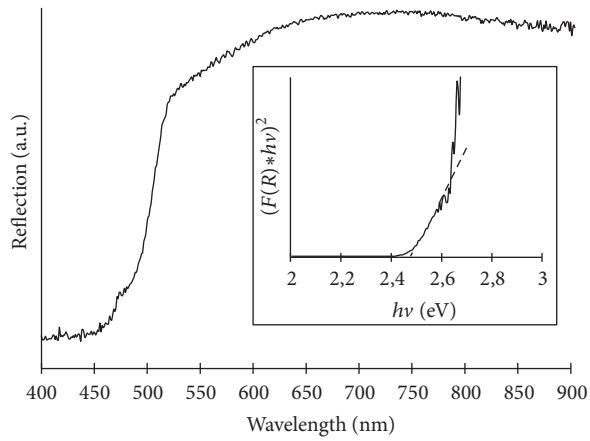

Figure 2: Reflectance diffuse spectra of In_2S_3 powder (Kubelka-Munk fitting as function of photon energy).

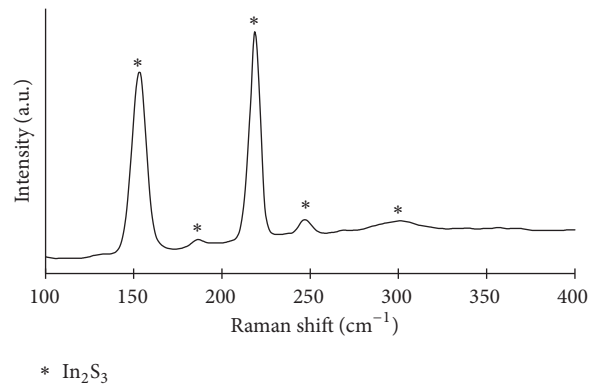

Figure 3: Raman spectra of In_2S_3 powder.

where R_α is the reflectance and $F(R_\alpha)$ is proportional to the absorption constant of the material, an indicative of the absorbance of the sample at a particular wavelength. For using Kubelka-Munk function (2) on the reflectance spectrum, we can obtain the graph of absorbance versus wavelength; Figure 2 shows the Kubelka-Munk function versus photon energy. The optical band gap of the films was determined by extrapolating the linear portion of $(F(R_\alpha)hv)^2$ versus hv plot on the x-axis.

$$\left(F\left(R_\alpha\right)hv\right)^2 = A\left(hv - E_g\right), \tag{3}$$

where "E_g" is the band gap energy and "A" is a constant depending on the transition probability.

Figure 2 (insight) shows that the band gap of the compound was 2.47 eV. All signals of diffraction pattern correspond to In_2S_3; however, this value is higher than the value reported to bulk In_2S_3 value of 2.07 eV; in CBD process precipitation of other phases (e.g., oxides and hydroxides) had been reported; if they are present in the catalyst, they can increase the band gap value. Furthermore, band gap value indicates that catalyst can be active in the visible region of the electromagnetic spectrum; if semiconductor absorbs visible radiation it could be useful for degrading pollutant for using direct solar radiation [21, 22].

3.3. Raman Spectroscopy Study. Figure 3 shows modes obtained by Raman spectra for catalyst powder; definition and intensity of the signal in Raman spectra revealed high crystalline quality of catalyst; this result is according to XRD pattern diffraction; Raman spectra show five normal modes of vibration at 155 cm^{-1}, 186 cm^{-1}, 218 cm^{-1}, 243 cm^{-1}, and 305 cm^{-1}; these signals can be assigned to modes of vibrations of In_2S_3 phase; signals located at 186 cm^{-1}, 243 cm^{-1}, and 305 cm^{-1} can be assigned to A_{1g} vibration modes of In_2S_3 phase; this result is according to other reports [23].

3.4. Adsorption Process. In relation to photocatalytic degradation, step of physical or chemical adsorption process prior to beginning of photodegradation step is a process poorly studied; it is well known that the adsorption of contaminant species on the surface of the photocatalyst is an important step prior to degradation process. In this study, Langmuir and Freundlich isotherm models were employed to describe the MB adsorption equilibrium. In Langmuir isotherm model, the adsorption process is taking place isothermally and adsorbent surface can be covered uniformly with a monolayer of adsorbate. The linear form of the Langmuir equation is

$$\frac{C_e}{q} = \frac{1}{q_m b} + \frac{C_e}{q_m}, \tag{4}$$

where C_e is the equilibrium concentration of dye; q is the amount of dye adsorbed per gram of catalyst; q_m represents the maximum amount of dye that can be adsorbed; and b is related to the adsorption rate. The linear form of the Freundlich equation is

$$\ln\left(q\right) = \ln\left(k\right) + \frac{1}{n}\ln C_{\text{eq}}, \tag{5}$$

where k is an indicator of adsorption capacity, as the higher the maximum capacity is, the higher the k value is; furthermore, ratio $(1/n)$ is a measure of intensity adsorption. The n and k values are empirical constants and they are specific to the system adsorbent/adsorbate [24].

Figure 4 shows the experimental results of adsorption equilibrium of different loads of MB on 0.25 g of In_2S_3 powder.

Figure 4 shows adsorption kinetics of MB over In_2S_3; results show that system reaches adsorption equilibrium point after 1 hour of dark agitation; from experimental results of Figure 4 and applying fitting of (4) and (5) we obtain adsorption isotherms for two theoretical models. Table 1 lists the fitting results and Figure 5 shows the experimental results of adsorption equilibrium of MB on In_2S_3 and theoretical fitting to Langmuir model. The fitting results indicated that the Langmuir isotherm describes the experimental results MB adsorption equilibrium.

3.5. Photocatalytic Test. Figure 6 shows change of molar fraction (x) of MB under both dark and visible irradiation.

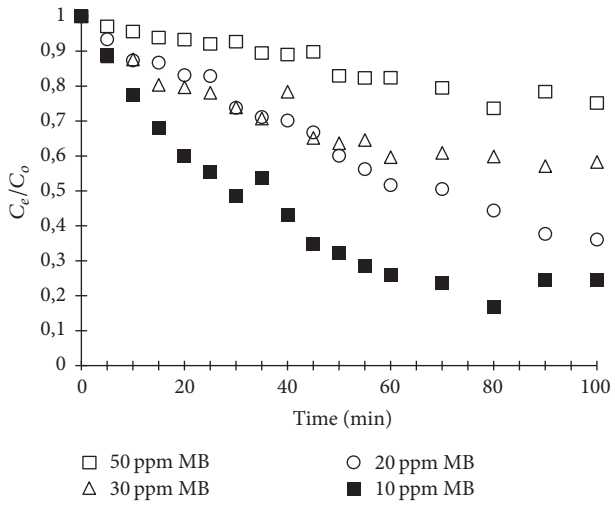

Figure 4: Adsorption process of In_2S_3 powder (0.025 g) at different MB loads.

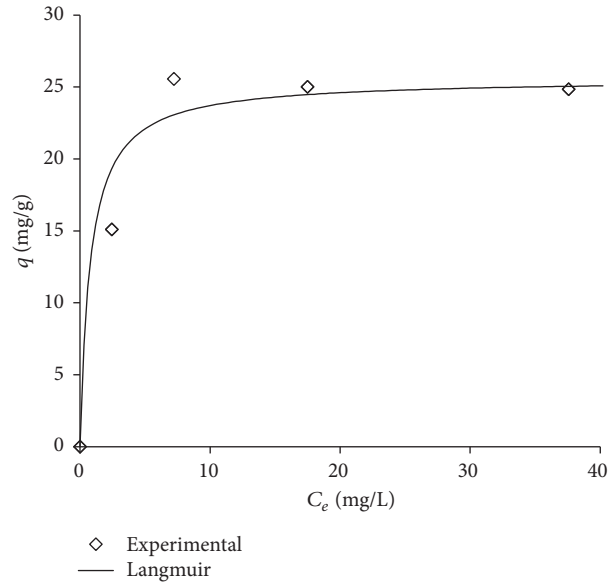

Figure 5: Langmuir and Freundlich model fitting to MB adsorption on In_2S_3 powder.

Table 1: Linear fitting experimental results.

Model	Parameter (unit)	Value
Langmuir	Q_m (mg/g)	25,3
	K (L/g)	0.7
	R^2	0.979
Freundlich	n	5.8
	k	3.2
	R^2	0.627

In_2S_3 adsorption on dark stirring occurs until 60 minutes; after that visible irradiation begins and significant increase in photocatalytic activity was observed. Adsorption and

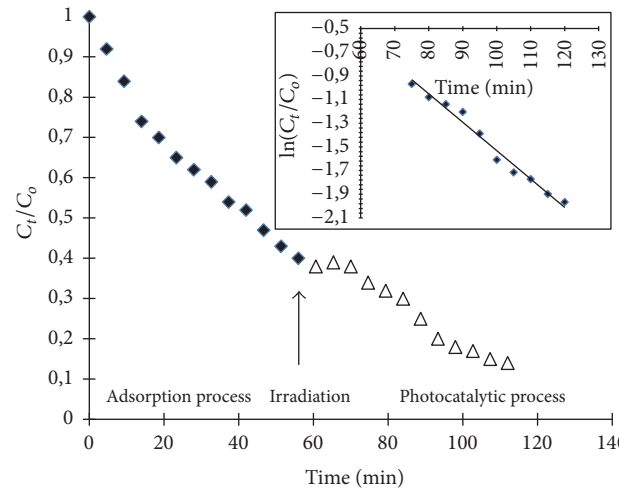

Figure 6: MB removal yield in dark stirring and under visible light irradiation.

photomineralization rate of methylene blue followed the Langmuir–Hinshelwood (L-H) kinetics model [25]:

$$v = -\frac{d\,[\mathrm{MB}]}{dt} = -\frac{kK\,[\mathrm{MB}]}{1 + K\,[\mathrm{MB}]}, \tag{6}$$

where v is the rate of dye mineralization, k is the rate constant, [MB] is the methylene blue concentration, and K is the adsorption coefficient. Equation (6) can be solved explicitly for (t) for using discrete changes in [MB] from the initial concentration to a zero reference point. In our case, an apparent first-order model can be assumed:

$$v = -\frac{d\,[\mathrm{MB}]}{dt} = k'\,[\mathrm{MB}] = kK\,[\mathrm{MB}]\,. \tag{7}$$

Integration result in ((6) and (7)) is as follows:

$$[\mathrm{MB}] = [\mathrm{MB}]_o\, e^{-k't}, \tag{8}$$

where (t) is time in minutes and k' is the apparent reaction rate constant (min^{-1}); the assumption of a pseudo-first-order model was used in several studies to characterize the effect of different experimental conditions on the degradation rate [26].

Figure 6 shows change of methylene blue removal yield both in dark stirring and under visible light illumination, inside; we show pseudo-first-order model fitting. Figure 6 shows after 60 minutes a plateau zone is reached, under dark stirring; after that under visible irradiation, system reaches 86% of MB concentration reduction; this 26% could be assigned to photocatalytic process. These results indicate that In_2S_3 has photocatalytic properties under visible irradiation. The k' value for In_2S_3 was established from the slope of the linear fitting of $\ln(\mathrm{MB}/\mathrm{MB}_o)$ versus time. We obtained a k' value of $2.4 \times 10^{-2}\ \mathrm{min}^{-1}$. This is a significant result due to possibility of using visible radiation directly under catalysts without physical or chemical modification as TiO_2 required to be photocatalytically active under visible irradiation.

4. Conclusions

We synthesized In_2S_3 by CBD process. Structural characterization indicated that catalyst powder was polycrystalline; besides, optical analysis indicated that compound was active in visible region of electromagnetic spectrum; it had a band gap of 2.47 eV. Furthermore, Langmuir adsorption model described equilibrium adsorption of MB on In_2S_3. Finally, In_2S_3 had photocatalytic activity on MB degradation; results indicated that MB load reduced 26% after visible illumination.

Conflicts of Interest

The authors declare that they have no conflicts of interest.

Acknowledgments

This research was supported by Universidad del Atlántico (Project Code CB20-FGI2016).

References

[1] M. Mehrjouei, S. Müller, and D. Möller, "A review on photocatalytic ozonation used for the treatment of water and wastewater," *Chemical Engineering Journal*, vol. 263, pp. 209–219, 2015.

[2] M. Juntti, D. Russel, and J. Turnpenny, "Evidence, politics and power in public policy for the environment," *Environmental Science and Policy*, vol. 12, no. 3, pp. 207–215, 2009.

[3] K. Annan, *Water for People, Water for Life, Executive Summary of the UN World Development Report*, UNESCO-WWAP, 2003.

[4] A. Ahmadi and L. Tiruta-Barna, "A process modelling-life cycle assessment-multiobjective optimization tool for the eco-design of conventional treatment processes of potable water," *Journal of Cleaner Production*, vol. 100, pp. 116–125, 2015.

[5] C. V. Gómez-Pacheco, J. Rivera-Utrilla, M. Sánchez-Polo, and J. J. López-Peñalver, "Optimization of the preparation process of biological sludge adsorbents for application in water treatment," *Journal of Hazardous Materials*, vol. 217-218, pp. 76–84, 2012.

[6] P. Wang, N. Xu, and J. Shi, "A pilot study of the treatment of waste rolling emulsion using zirconia microfiltration membranes," *Journal of Membrane Science*, vol. 173, no. 2, pp. 159–166, 2000.

[7] R. Tarpagkou and A. Pantokratoras, "The influence of lamellar settler in sedimentation tanks for potable water treatment—a computational fluid dynamic study," *Powder Technology*, vol. 268, no. 1, pp. 139–149, 2014.

[8] E. Repo, M. Mäkinen, S. Rengaraj, G. Natarajan, A. Bhatnagar, and M. Sillanpää, "Lepidocrocite and its heat-treated forms as effective arsenic adsorbents in aqueous medium," *Chemical Engineering Journal*, vol. 180, pp. 159–169, 2012.

[9] D. Li, Q. Zhu, C. Han, Y. Yang, W. Jiang, and Z. Zhang, "Photocatalytic degradation of recalcitrant organic pollutants in water using a novel cylindrical multi-column photoreactor packed with TiO_2-coated silica gel beads," *Journal of Hazardous Materials*, vol. 285, pp. 398–408, 2015.

[10] B. A. Wols and C. H. M. Hofman-Caris, "Review of photochemical reaction constants of organic micropollutants required for UV advanced oxidation processes in water," *Water Research*, vol. 46, no. 9, pp. 2815–2827, 2012.

[11] Z. Wang, X. Liu, W. Li, H. Wang, and H. Li, "Enhancing the photocatalytic degradation of salicylic acid by using molecular imprinted S-doped TiO_2 under simulated solar light," *Ceramics International*, vol. 40, no. 6, pp. 8863–8867, 2014.

[12] M. V. Dozzi and E. Selli, "Doping TiO_2 with p-block elements: effects on photocatalytic activity," *Journal of Photochemistry and Photobiology C: Photochemistry Reviews*, vol. 14, no. 1, pp. 13–28, 2013.

[13] G. R. Gopinatha, R. W. Milesb, and K. T. R. Reddya, "Influence of bath temperature on the properties of In_2S_3 films grown by chemical bath deposition," *Energy Procedia*, vol. 34, pp. 399–406, 2013.

[14] W. Wang, G. Huang, J. C. Yu, and P. K. Wong, "Advances in photocatalytic disinfection of bacteria: development of photocatalysts and mechanisms," *Journal of Environmental Sciences*, vol. 34, pp. 232–247, 2015.

[15] T. Sall, B. M. Soucase, M. Mollar, B. Hartitti, and M. Fahoume, "Chemical spray pyrolysis of β-In_2S_3 thin films deposited at different temperatures," *Journal of Physics and Chemistry of Solids*, vol. 76, pp. 100–104, 2015.

[16] R. Lucena, F. Fresno, and J. C. Conesa, "Spectral response and stability of In_2S_3 as visible light-active photocatalyst," *Catalysis Communications*, vol. 20, pp. 1–5, 2012.

[17] J. Chen, W. Liu, and W. Gao, "Tuning photocatalytic activity of In_2S_3 broadband spectrum photocatalyst based on morphology," *Applied Surface Science*, vol. 368, pp. 288–297, 2016.

[18] R. Bayón and J. Herrero, "Structure and morphology of the indium hydroxy sulphide thin films," *Applied Surface Science*, vol. 158, no. 1, pp. 49–57, 2000.

[19] N. Revathi, P. Prathap, and K. T. R. Reddy, "Synthesis and physical behaviour of In_2S_3 films," *Applied Surface Science*, vol. 254, no. 16, pp. 5291–5298, 2008.

[20] M. Burgos and M. Langlet, "The sol-gel transformation of TIPT coatings: a FTIR study," *Thin Solid Films*, vol. 349, no. 1-2, pp. 19–23, 1999.

[21] P. Roy, J. R. Ota, and S. K. Srivastava, "Crystalline ZnS thin films by chemical bath deposition method and its characterization," *Thin Solid Films*, vol. 515, no. 4, pp. 1912–1917, 2006.

[22] N. Naghavi, R. Henriquez, V. Laptev, and D. Lincot, "Growth studies and characterisation of In_2S_3 thin films deposited by atomic layer deposition (ALD)," *Applied Surface Science*, vol. 222, no. 1–4, pp. 65–73, 2004.

[23] E. Kärber, K. Otto, A. Katerski, A. Mere, and M. Krunks, "Raman spectroscopic study of In_2S_3 films prepared by spray pyrolysis," *Materials Science in Semiconductor Processing*, vol. 25, pp. 137–142, 2014.

[24] J. E. House, *Principles of Chemical Kinetics*, Elsevier Press, 2007.

[25] P. Simoncic and T. Armbruster, "Cationic methylene blue incorporated into zeolite mordenite-Na: a single crystal X-ray study," *Microporous and Mesoporous Materials*, vol. 81, no. 1–3, pp. 87–95, 2005.

[26] T. Zhang, T. Oyama, A. Aoshima, H. Hidaka, J. Zhao, and N. Serpone, "Photooxidative *N*-demethylation of methylene blue in aqueous TiO_2 dispersions under UV irradiation," *Journal of Photochemistry and Photobiology A: Chemistry*, vol. 140, no. 2, pp. 163–172, 2001.